Controlling the range of interactions in the classical inertial ferromagnetic Heisenberg model:

analysis of metastable states

Controlling the range of interactions in the classical inertial ferromagnetic Heisenberg model: analysis of metastable states

Leonardo J L Cirto[1], Leonardo S Lima[2] and Fernando D Nobre[1,3]

[1] Centro Brasileiro de Pesquisas Físicas, Rua Xavier Sigaud 150, 22290-180, Rio de Janeiro—RJ, Brazil
[2] Departamento de Física e Matemática, Centro Federal de Educação Tecnológica de Minas Gerais, 30510-000, Belo Horizonte—MG, Brazil
[3] National Institute of Science and Technology for Complex Systems, Rua Xavier Sigaud 150, 22290-180, Rio de Janeiro—RJ, Brazil
E-mail: cirto@cbpf.br, lslima@des.cefetmg.br and fdnobre@cbpf.br

Abstract. A numerical analysis of a one-dimensional Hamiltonian system, composed by N classical localized Heisenberg rotators on a ring, is presented. A distance r_{ij} between rotators at sites i and j is introduced, such that the corresponding two-body interaction decays with r_{ij} as a power-law, $1/r_{ij}^{\alpha}$ ($\alpha \geqslant 0$). The index α controls the range of the interactions, in such a way that one recovers both the fully-coupled (i.e. mean-field limit) and nearest-neighbour-interaction models in the particular limits $\alpha = 0$ and $\alpha \to \infty$, respectively. The dynamics of the model is investigated for energies U below its critical value ($U < U_c$), with initial conditions corresponding to zero magnetization. The presence of quasi-stationary states (QSSs), whose durations t_{QSS} increase for increasing values of N, is verified for values of α in the range $0 \leqslant \alpha < 1$, like the ones found for the similar model of XY rotators. Moreover, for a given energy U, our numerical analysis indicates that $t_{\mathrm{QSS}} \sim N^{\gamma}$, where the exponent γ decreases for increasing α in the range $0 \leqslant \alpha < 1$ and particularly, our results suggest that $\gamma \to 0$ as $\alpha \to 1$. The growth of t_{QSS} with N could be interpreted as a

breakdown of ergodicity, which is shown herein to occur for any value of α in this interval.

Contents

1. Introduction

Classical spin models have called the attention of statistical-mechanics and magnetism researchers throughout many years [1–5]. Many techniques have been used in their study, both analytical and numerical, in such a way that a reasonable knowledge of their equilibrium thermodynamics has been achieved and specially, of their critical properties. Among those models, one could mention the n-vector classical spin models, which present the XY ($n = 2$) and Heisenberg ($n = 3$) as particular cases.

An interesting formulation of a n-vector classical model comes when one adds a kinetic term to its Hamiltonian, i.e. the spin variables may be interpreted as classical rotators (see, e.g. [6–8]), so that the terminology 'inertial model' is currently used. This additional term does not pose difficulties in the calculation of equilibrium properties within a canonical-ensemble approach, but it turns possible to derive equations of motion for each rotator, which can be integrated by means of a molecular-dynamics procedure. In this way, the dynamical behaviour of these models can be investigated numerically without the need of introducing any particular type of probabilistic transition rules for changing the microscopic states.

The inertial ferromagnetic XY model was introduced in [6], within a fully-coupled framework (i.e. infinite-range interactions), a limit where the mean-field approach becomes exact. Mostly referred to as 'Hamiltonian Mean Field' (HMF) model, it became

paradigmatic in the study of the dynamical behaviour of classical many-body Hamiltonian systems and it has given rise to a large amount of works [9–18]. One of the most interesting features in the HMF model concerns the appearance of metastable states, for some particular initial conditions, whose lifetime grows by increasing the total number of rotators, that could be interpreted as a breakdown of ergodicity in the thermodynamic limit.

A generalization of the HMF model was proposed in [7], by introducing a distance r_{ij} between rotators at sites i and j of a given lattice. Moreover, the two-body interaction was assumed to decay with r_{ij}, like a power-law, $1/r_{ij}^\alpha$ ($\alpha \geqslant 0$). The index α controls the range of the interactions, in such a way that one recovers both the HMF and nearest-neighbour-interaction models in the particular limits $\alpha = 0$ and $\alpha \to \infty$, respectively. In between these two limits, one finds an important change of behaviour in the thermodynamic quantities, yielding two physically distinct regimes, namely, the long- ($\alpha \leqslant d$) and short-range ($\alpha > d$) interaction regimes [7, 19–21]. In the latter, one has the usual extensive and intensive quantities, whereas in the former, one may find also nonextensive thermodynamic quantities [22]. This generalization is usually referred to as α-XY or α-HMF model and it also has been studied by several groups [17, 20, 21, 23–25].

The dynamics of the fully-coupled inertial version of the ferromagnetic Heisenberg model has been much less investigated in the literature [8, 26, 27]. Metastable, or quasi-stationary states (QSSs), also occur for this system, similar to those that appear in the HMF model; their lifetime diverge by increasing the total number of rotators N, which implies that the order in which the thermodynamic limit ($N \to \infty$) and the infinite-time limit ($t \to \infty$) are considered, becomes important. More specifically, if we let $N \to \infty$ first, the system remains trapped in these QSSs, never reaching the final Boltzmann–Gibbs (BG) equilibrium state, most probably being the QSS itself the final state in such a case. In these metastable states, thermodynamical quantities, like temperature and magnetization, do not coincide with the canonical-ensemble predictions.

Herein, we will modify the fully-coupled inertial ferromagnetic Heisenberg model, by introducing a distance r_{ij} between rotators at sites i and j of a given lattice. Analogously to the α-HMF model [7], the rotator–rotator interaction will be taken to decay with the distance like a power-law, $1/r_{ij}^\alpha$ ($\alpha \geqslant 0$). The interaction part of this Hamiltonian has already been studied analytically in [28], within a canonical-ensemble approach to the equilibrium state of the corresponding d-dimensional model, where it was shown that if the two-body interaction is appropriately scaled, a universal thermodynamical behaviour is achieved for $0 \leqslant \alpha < d$, e.g. relations involving temperature T, magnetization M and internal energy U become α-independent in this interval. Apart from this study of the equilibrium state, an investigation of the dynamical behaviour of the above-mentioned Heisenberg model and particularly, how the QSSs may be affected by the exponent α, has never been addressed in the literature, to our knowledge. In the present work we study this model on a ring, i.e. $d = 1$ with periodic boundary conditions, using molecular-dynamics simulations. We perform a detailed analysis of the QSSs behaviour by varying the energy, number of particles and range of the interaction, i.e. the exponent α. In the next section we define the model, the appropriate scaling for the interactions, the canonical-ensemble solution, equations of motion and initial conditions to be used in the molecular-dynamics procedure. In section 3 we present the results of our simulations, showing an agreement with some analytical results known in the literature for the equilibrium state,

in some particular limits; most importantly, we show the existence of QSSs for energies U below criticality ($U < U_\mathrm{c}$). Such QSSs, which were verified herein for initial conditions corresponding to zero magnetization, appear for values of α in the range $0 \leqslant \alpha < 1$, being characterized by durations t_QSS that increase for increasing values of N, like those found numerically and analytically in previous works of the similar model of XY rotators [9–18, 24, 29, 30]. Finally, in section 4 we present our main conclusions.

2. The model

First, let us define the model in terms of N localized interacting classical rotators, on a d-dimensional hypercubic lattice, through the Hamiltonian

$$\mathcal{H} = \frac{1}{2} \sum_{i=1}^{N} \mathbf{L}_i^2 + \frac{1}{2\widetilde{N}} \sum_{i=1}^{N} \sum_{\substack{j=1 \\ j \neq i}}^{N} \frac{1 - \mathbf{S}_i \cdot \mathbf{S}_j}{r_{ij}^{\alpha}} = K + V \ , \tag{1}$$

where $\alpha \geqslant 0$ and $\mathbf{S}_i$ represents a vector with $n = 3$ components, assigned to the rotator at site i (similar to a classical Heisenberg spin variable), allowed to change its direction continuously inside a 3-dimensional sphere of unity radius, leading to the constraint $\mathbf{S}_i \cdot \mathbf{S}_i = S_i^2 = 1$ ($\forall\, i$)[4]. Moreover, $\mathbf{L}_i$ depicts the corresponding angular momentum (we are considering moments of inertia equal to unit, so that angular momenta and angular velocities are equivalent quantities). The coupling constants may be identified as $J_{ij} = 1/(\widetilde{N} r_{ij}^{\alpha})$, where r_{ij} measures the (dimensionless) distance between rotators i and j, defined as the minimal one, given that periodic boundary conditions will be considered.

One should notice that the interaction term defined in equation (1) is long-ranged for $\alpha \leqslant d$, in the sense that if $\widetilde{N} \sim \mathcal{O}(1)$ the partition function does not admit a well-defined thermodynamic limit [28], e.g. the internal energy per particle diverges in the limit $N \to \infty$, so that the system is said to be nonextensive [22]. Consequently, in order to calculate the thermodynamic limit adequately whenever $\alpha \leqslant d$, the quantity $\widetilde{N}$ has to be defined appropriately to ensure a total energy proportional to the system size N. For $\alpha = 0$ this is attained with $\widetilde{N} = N$, the so-called Kac's prescription [4,5,17,28]. For a general $0 \leqslant (\alpha/d) < \infty$, the extensivity of the Hamiltonian in (1) is achieved through the following choice for $\widetilde{N}$,

$$\widetilde{N} \equiv \frac{1}{N} \sum_{i=1}^{N} \sum_{\substack{j=1 \\ j \neq i}}^{N} \frac{1}{r_{ij}^{\alpha}}. \tag{2}$$

This may be seen intuitively if we note that for N large, $\widetilde{N} \sim N^{1-\alpha/d}$, if $0 \leqslant (\alpha/d) < 1$ (hence, $\widetilde{N} \sim N$ for $\alpha = 0$), $\widetilde{N} \sim \ln N$, if $(\alpha/d) = 1$ and $\widetilde{N} \sim 1/(\alpha/d - 1) \sim \mathcal{O}(1)$, if $(\alpha/d) > 1$; therefore, this proposal yields the interaction term in the Hamiltonian (1) proportional to the system size N, for all $\alpha \geqslant 0$.

The need of the scaling in equation (2), for systems characterized by long-range interactions, began to be realized within a generalized ferrofluid model [19] (see also [31]). This proposal was applied successfully to a controllable-range interaction (α-dependent)

---

[4] This constraint reduces the number of degrees of freedom per particle from three to two.

Curie–Weiss model, where it was shown numerically that by considering such a scaling, the magnetization per particle follows a thermodynamical equation of state, $M = M(T)$, that becomes independent of α in the nonextensive regime [32]. Moreover, applications of this scaling for Lennard–Jones-like systems were carried in [33]. In addition to the aforementioned works, the correctness of the conjectural scaling of equation (2) has been verified in several other systems, suggesting that it should be valid for a wide variety of systems with long-range interactions [22].

A systematic analysis of equation (2) has been particularly undertaken for the α-XY model [7], whose Hamiltonian is identical to equation (1), but $n = 2$, i.e. $\mathbf{S}_i$ is treated as a two-dimensional classical rotator, allowed to change its direction continuously inside a circle of unit radius. For this system, it was shown both analytically [23, 28] and numerically [21, 23, 24, 30] that, for $0 \leqslant \alpha < d$, the prescription (2) associates to the α-XY model the same thermodynamical behaviour as the one previously known for the case $\alpha = 0$ [6]. Furthermore, the work of [28] has extended such a result to a general n-dimensional $\mathbf{S}_i$ ($n = 1, 2, \ldots$) unit vector.

Although the model of equation (1) has been defined on a d-dimensional hypercubic lattice, from now on we will restrict ourselves to a ring, i.e. a one-dimensional chain with periodic boundary conditions. Based on its successful use for the above-mentioned systems, we will consider the scaling of equation (2) for the present problem as well.

2.1. The canonical-ensemble solution

Within a canonical-ensemble solution, the kinetic term K of the Hamiltonian in equation (1) does not bring difficulties in the evaluation of average values. Hence, the nontrivial part for the calculation of equilibrium properties of the Hamiltonian (1) comes from the interaction term V. This term may become troublesome to deal analytically for dimensions $d > 1$ and to our knowledge, it has been investigated analytically only for $d = 1$, i.e. the linear chain, in some particular regimes of α, namely, $\alpha < d$ and $\alpha \to \infty$. The model on an open linear chain with nearest-neighbour interactions (limit $\alpha \to \infty$) was solved exactly in [1], whose solution is equivalent to the one considering periodic boundary conditions, in the thermodynamic limit [2] (see also [4,5,34]). On the other hand, the fully-coupled limit ($\alpha = 0$) corresponds to the case where the mean-field approach becomes exact, so that the model may be solved through a relatively easy calculation (see, e.g. [8]). As mentioned above, using the scaling of equation (2) the solution for $\alpha = 0$ applies to all $0 \leqslant \alpha < d$ [28].

Therefore, considering the model of Hamiltonian (1) defined on a ring, i.e. a one-dimensional chain with periodic boundary conditions, the solutions described above may be summarized, yielding for the internal energy and magnetization per particle respectively (we work with units such that $k_{\mathrm{B}} = 1$),

$$U(M, T) = \begin{cases} T + \frac{1}{2}\left[1 - L^2(M/T)\right] & ; \quad \text{if } 0 \leqslant \alpha < 1 , \\ T + \frac{1}{2}\left[1 - L(1/2T)\right] & ; \quad \text{if } \alpha \to \infty , \end{cases} \tag{3}$$

$$M(T) = \begin{cases} M = L(M/T) & ; \quad \text{if } 0 \leqslant \alpha < 1 , \\ M = 0 & ; \quad \text{if } \alpha \to \infty , \end{cases} \tag{4}$$
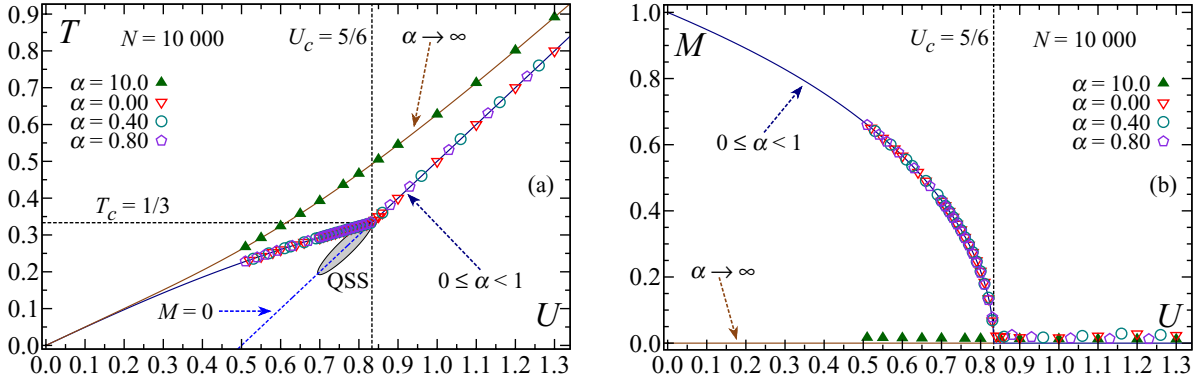
Figure 1. The good agreement between the analytical results [full lines, see equations (3) and (4)] and data from numerical simulations of a system composed by $N = 10\,000$ rotators, in the long-time limit (symbols), is presented for the controllable-range inertial Heisenberg model defined by equation (1). (a) The kinetic temperature $T = \langle K(t)\rangle_{\text{time}}/N$ (which coincides with the temperature T at equilibrium) versus the internal energy U; (b) The magnetization M versus the internal energy U. In panel (a) (in panel (b)) we compare numerical data, for typical values of α, with the caloric curves (with the magnetization curve) in the cases $0 \leqslant \alpha < 1$ [8, 28], as well as in the limit $\alpha \to \infty$ [1, 2]. In the former case, one has a second-order phase transition at the critical point $(T_c = 1/3, U_c = 5/6)$ (dashed lines), separating the ferromagnetic $(U < U_c)$ and paramagnetic $(U > U_c)$ phases. The metastable solution corresponding to the quasi-stationary state (QSS) that appears for $U < U_c$, characterized by zero magnetization (shaded region) and presenting a lower kinetic temperature than the corresponding equilibrium solution, is also represented.

where $M(T)$ denotes the modulus of the magnetization vector,

$$\mathbf{M} = \frac{1}{N}\sum_{i=1}^{N}\mathbf{S}_i \ . \tag{5}$$

In these equations, $L(x)$ represents the Langevin function,

$$L(x) = \coth x - \frac{1}{x} = \frac{I_{3/2}(x)}{I_{1/2}(x)} \ ,$$

and $I_n(x)$ is the modified Bessel function of the first kind.

The analytical results presented above are displayed as solid lines in figure 1, where one finds a continuous phase transition separating the ferromagnetic and paramagnetic states for values of α in the interval $0 \leqslant \alpha < 1$; for $\alpha \to \infty$, there is no phase transition at a finite temperature, so that only the disordered phase with $M = 0$ exists. In the first case, at sufficiently high temperatures (or equivalently, high enough energies), the directions of the $\{\mathbf{S}_i\}$ become randomly distributed, corresponding to the paramagnetic disordered phase, where one has the order parameter $M = 0$. At the fundamental state all spins are parallel, corresponding to the ferromagnetically fully ordered case with $M = 1$. Hence, for all cases $0 \leqslant \alpha < 1$, in between these two regimes, a continuous phase transition occurs at a critical temperature $T_c = 1/3$, with an associated critical energy $U_c = 5/6 \approx 0.833$.

2.2. Equations of motion

Herein we work with Cartesian components for the spin variables and angular momenta, written respectively as $\mathbf{S}_i = (S_{x_i}, S_{y_i}, S_{z_i})$ and $\mathbf{L}_i = (L_{x_i}, L_{y_i}, L_{z_i})$, yielding 6 variables for each rotator. Hence, the set of $6N$ equations to be solved numerically can be cast in the following form [35],

$$\dot{\mathbf{L}}_i = \mathbf{S}_i \times \left[\frac{1}{\widetilde{N}} \sum_{\substack{j=1 \\ j \neq i}}^{N} \frac{\mathbf{S}_j}{r_{ij}^{\alpha}} \right] , \tag{6}$$

$$\dot{\mathbf{S}}_i = \mathbf{L}_i \times \mathbf{S}_i , \tag{7}$$

for $i = 1, 2, \ldots, N$. One notices that, in the particular case $\alpha = 0$, the expression for $\dot{\mathbf{L}}_i$ used in previous works [8,26] is recovered, namely, $\dot{\mathbf{L}}_i = \mathbf{S}_i \times \mathbf{M}$ [where $\mathbf{M}$ represents the magnetization per particle of equation (5)].

It is important to remind that equations (6) and (7), written in the Cartesian representation, are not canonical equations of motion, since S_{μ_i} and L_{μ_i} ($\mu = x, y, z$) do not represent canonically conjugate pairs. Alternatively, one could also work along the line of [27,36], by using spherical coordinates in order to write the spin variable as $\mathbf{S}_i = (\cos\varphi_i \sin\theta_i, \sin\varphi_i \sin\theta_i, \cos\theta_i)$ and the squared angular momentum in the corresponding Lagrangian as $\mathbf{L}_i^2 = L_{\theta_i}^2 + L_{\varphi_i}^2 / \sin^2\theta_i$. In this representation, one can derive equations of motion through the usual Hamiltonian formalism, where each rotator is characterized by two angles, $\theta_i \in [0, \pi)$ and $\varphi_i \in [0, 2\pi)$ and their canonically conjugate momenta, L_{θ_i} and L_{φ_i}. Although the use of spherical coordinates, instead of the Cartesian ones of equations (6) and (7), seems to be a natural way to handle the problem, the denominator $\sin^2\theta_i$ that appears in $\mathbf{L}_i^2$ becomes hard to be tackled numerically. Indeed, as $\sin\theta_i$ approaches zero, one needs to decrease the time step used in the integrations of the equations of motion, in such a way that the computational time may increase substantially. This difficulty has been discussed in the literature by several authors [37–39], where numerical techniques for circumventing it were proposed.

Based on the above-mentioned reasons, herein we shall deal with the equations of motion expressed in terms of Cartesian components, as in equations (6) and (7). It is straightforward to verify that, in addition to the total energy, the total angular momentum, $\mathbf{L} = \sum_{i=1}^{N} \mathbf{L}_i$, as well as the norm of each spin, $S_i = [\mathbf{S}_i \cdot \mathbf{S}_i]^{1/2}$, are also integrals of motion. Indeed, evaluating the time derivative of S_i and taking into account that $\dot{\mathbf{S}}_i \perp \mathbf{S}_i$, we get

$$\frac{\mathrm{d}S_i}{\mathrm{d}t} = \frac{\dot{\mathbf{S}}_i \cdot \mathbf{S}_i}{S_i} = 0 .$$

Similarly for $\dot{\mathbf{L}}$,

$$\sum_{i=1}^{N} \dot{\mathbf{L}}_i = \left(\sum_{i=1}^{N} \mathbf{S}_i \right) \times \left(\frac{1}{\widetilde{N}} \sum_{j=1}^{N} \frac{\mathbf{S}_j}{r_{ij}^{\alpha}} \right) = 0 .$$

It should be stressed that the equation of motion (6) corresponds precisely to the Euler equation for a linear rigid body of unit length (and unit inertial moments). In such system the angular momentum $\mathbf{L}_i$ is always perpendicular to $\mathbf{S}_i$ (the 'molecular' axis), yielding

the constraint $\mathbf{L}_i \cdot \mathbf{S}_i = 0$, to be incorporated in the initial state. Once this additional constraint is imposed, it will hold throughout the whole time evolution, since the product $\mathbf{L}_i \cdot \mathbf{S}_i$ is also a constant of motion, as we can verify by using equations (6) and (7),

$$\frac{\mathrm{d}}{\mathrm{d}t}\left(\mathbf{L}_i \cdot \mathbf{S}_i\right) = \dot{\mathbf{L}}_i \cdot \mathbf{S}_i + \mathbf{L}_i \cdot \dot{\mathbf{S}}_i = 0 \ . \tag{8}$$

2.3. Numerical procedure and initial conditions

All our molecular-dynamical simulations were carried for a single copy of the system defined by equation (1), considering fixed values of the total number of rotators N and energy per particle U. Since we are applying periodic boundary conditions, the model of equation (1) becomes defined on a ring, with r_{ij} corresponding to the minimal dimensionless distance between rotators i and j, taking the values $1, 2, 3 \ldots N/2$, for each rotator i. To integrate the $6N$ equations of motion (equations (6) and (7)) we have used a standard fourth-order Runge–Kutta scheme, with an integration step chosen in such a way to yield conservation of the energy per particle within a relative fluctuation smaller than 10^{-5}; this was achieved with a time step typically[5] of $\delta t = 0.02$.

The initial conditions used were such that each angular momentum component L_{μ_i} ($\mu = x, y, z$) was drawn at random from a uniform distribution and then rescaled to yield zero total angular momentum for the whole system. In what concerns the variables S_{μ_i}, the initial conditions corresponded to those of zero magnetization, achieved numerically as $M \approx 0$ (typically $\sim 10^{-3}$). For this, the components S_{x_i} and S_{y_i} were also drawn at random from a uniform distribution within the interval $[-1, 1]$, whereas the components S_{z_i} were set in such way to preserve the constraint $\mathbf{L}_i \cdot \mathbf{S}_i = 0$ ($\forall i$), i.e. through[6] $S_{z_i} = -\left(L_{x_i} S_{x_i} + L_{y_i} S_{y_i}\right)/L_{z_i}$. This procedure leads to unnormalized spins, which are then normalized by dividing each component by $\sqrt{S_{x_i}^2 + S_{y_i}^2 + S_{z_i}^2}$; finally, all L_{μ_i}'s were rescaled again to obtain precisely the desired total energy U. Consistently with equations (3) and (4), initial configurations with zero magnetization like the one just described above, only applies to a total energy $U > 1/2$.

3. Results

Although we are dealing with three Cartesian components for the angular momenta (L_{x_i}, L_{y_i} and L_{z_i}), due to the constraint $\mathbf{L}_i \cdot \mathbf{S}_i = 0$ only two of these components are independent. Let us then define the instantaneous kinetic temperature as given by $T(t) = K(t)/N$. Since we are working with a single copy of the system defined by equation (1), the time average at the equilibrium state should be identified with the thermodynamic temperature, $T = \langle T(t) \rangle_{\text{time}}$ and in a similar way, one has for the equilibrium magnetization, $M = \langle M(t) \rangle_{\text{time}}$. As it will be shown later on, such time averages should be computed after a sufficiently long time, where both $T(t)$ and $M(t)$

---

[5] A substantial gain in computational time was obtained, in the simulations with $\alpha \neq 0$ and larger values of N, by using a Fast-Fourier-Transform algorithm. To implement this technique we have used the FFTW library www.fftw.org.

[6] It should be mentioned that this constraint was not used in [8, 26], so that $\mathbf{L}_i \cdot \mathbf{S}_i = \delta_i$ ($\delta_i \in [-1, 1]$) in these works, at the beginning of the simulations. However, it was verified numerically that δ_i was also a constant of motion, in such a way that equation (8) remained true ($\forall i$).

fluctuate around the values predicted by Boltzmann–Gibbs (BG) statistical mechanics. In this regime, where ergodicity is expected to hold, time averages and ensemble averages should coincide.

In figure 1 we present results from analytical calculations (full lines) and data from numerical simulations in the long-time limit (symbols), for the controllable-range inertial Heisenberg model of equation (1). In figure 1(a) we represent the kinetic temperature versus the internal energy U, whereas in figure 1(b) we do the same for the magnetization. As mentioned above, at equilibrium, an average over the quantity $T(t)$ is expected to coincide with the temperature T (obtained from the equipartition theorem), so that for the analytical results presented, the vertical axis of figure 1(a) corresponds precisely to the equilibrium temperature T, whereas for the numerical ones, it represents the quantity computed from a time average. All data shown in figure 1 for both temperature and magnetization coincide with the analytical results, showing that the equilibrium state considered numerically should be the one predicted by BG theory. The canonical-ensemble solution of the case $\alpha = 0$ (see, e.g. [8]) is represented by the full line in figure 1(a) (usually known as the caloric curve), presenting a discontinuity in its slope at the critical point $(T_c = 1/3, U_c = 5/6)$, where the magnetization becomes zero. According to [28], the equilibrium analytical solution of the case $\alpha = 0$ should apply to any $0 \leqslant \alpha < 1$, so that the corresponding full lines in figures 1(a) and (b) hold for any α in this range. Such a universal behaviour was verified numerically for the α-XY model [21, 23, 24, 30] and it is now established herein for the Heisenberg model, as displayed in figure 1 for typical values of $0 \leqslant \alpha < 1$. For completeness, in figure 1(a) we also present the solution corresponding to the quasi-stationary state (QSS) hat appears for $U < U_c$, characterized by zero magnetization, leading to $T = U - 1/2$ and presenting a lower kinetic temperature than the corresponding equilibrium solution. It was essentially within the energy range $0.70 \lesssim U < U_c = 5/6$ that QSSs have been investigated within the present numerical investigation. In the limit $\alpha \to \infty$ our model recovers the nearest-neighbour-interaction inertial Heisenberg model on a linear chain, for which the interaction part was solved exactly in [1, 2] and shown to present zero magnetization for all $T > 0$; consequently, its caloric curve exhibits the smooth behaviour indicated in figure 1(a). In this case, our simulations for $\alpha = 10$ are in full agreement with the results of the analytical solutions.

In figure 2 we exhibit the time evolution of $T(t)$ (conveniently rescaled in each case by the corresponding equilibrium temperature T_{BG}) for typical values of energies, $U < U_c = 5/6 \approx 0.833$ and $\alpha = 0.0, 0.4$ and 0.8. Simulations were carried for a single copy of $N = 10\,000$ rotators, considering the above-defined initial conditions, for sufficiently long times (up to times slightly larger than $t = 10^7$ in some cases). For all energies investigated, in the range $0.70 \leqslant U \leqslant 0.83$, we have verified the existence of QSSs and after these, a crossover is observed to a state whose temperature and magnetization coincide with those obtained analytically within BG statistical mechanics. For a given value of α one has that: (i) The lower energies have produced QSSs with smaller durations t_{QSS} and one observes that t_{QSS} increases substantially as one approaches the critical energy; (ii) The gaps separating $T(t)$ of these QSSs and their corresponding values of equilibrium temperatures T_{BG} are larger for smaller energies, dropping to zero as $U \to U_c$. On the other hand, for a fixed total energy, higher values of α yield smaller t_{QSS} and it will be shown later on that these durations tend to zero as $\alpha \to 1$. Therefore, the QSSs disappear in both limits $U \to U_c$ and $\alpha \to 1$. The existence of QSSs for energies below, but sufficiently
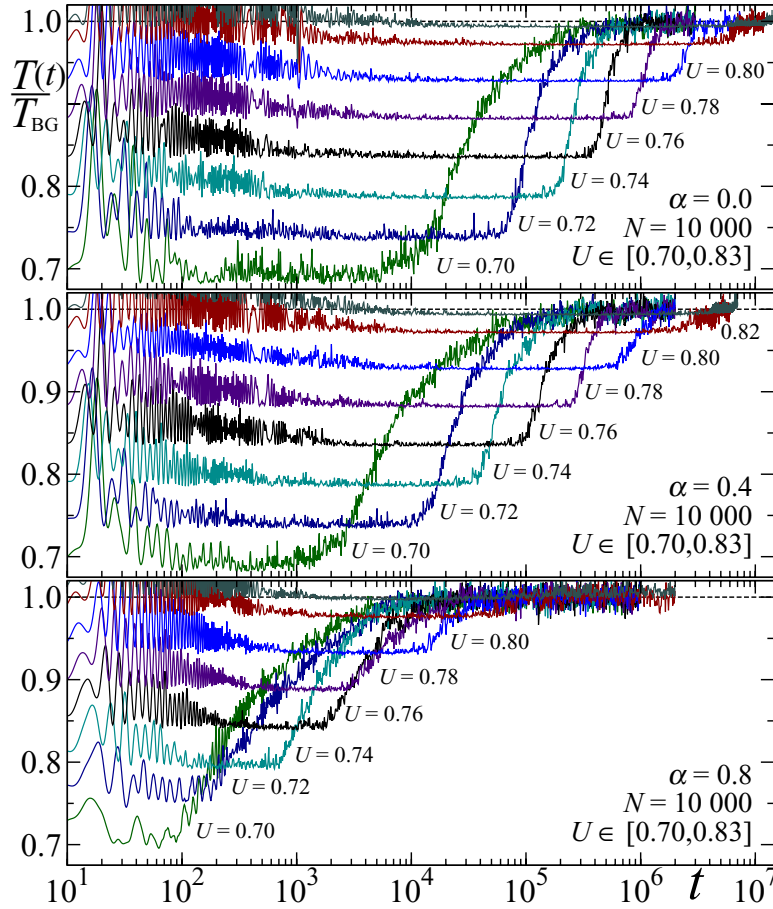
Figure 2. Time evolution of the dimensionless quantity $T(t)/T_{\mathrm{BG}}$ for typical values of the total energy U ($U < U_c$), for a single copy of $N = 10\,000$ Heisenberg rotators, in the cases $\alpha = 0.0, 0.4$ and 0.8 (from top to bottom). For each value of U, the corresponding equilibrium temperature T_{BG} is obtained from the caloric curve in figure 1. The time is also dimensionless and each unit of (physical) time t corresponds to 50 iterations of the equations of motion.

close to U_c, is well known to occur in the HMF and α-XY (with $0 < \alpha < 1$) models and it has been found analytically and numerically by many authors [9–18, 24, 29, 30]. Moreover, the most interesting characteristic of such states concerns an increase in their lifetime with the total number of rotators N; this property will also be verified for the present model.

The QSSs shown in figure 2 appear throughout the whole range $0 \leqslant \alpha < 1$, as exhibited in figure 3 for several values of α. Each case corresponds to molecular-dynamics simulations of a single realization of $N = 10\,000$ Heisenberg rotators defined by equation (1), with a total energy $U = 0.76$. One sees that the lifetime of these QSSs decrease for increasing values of α in the range $0 \leqslant \alpha < 1$ and that all QSSs occur at a kinetic temperature corresponding to zero magnetization (or slightly larger than zero), i.e. $T \gtrsim U - 1/2 = 0.26$. After these QSSs, the system approaches the BG equilibrium temperature ($T_{\mathrm{BG}} \approx 0.3118$), associated to its energy through the caloric curve of figure 1.
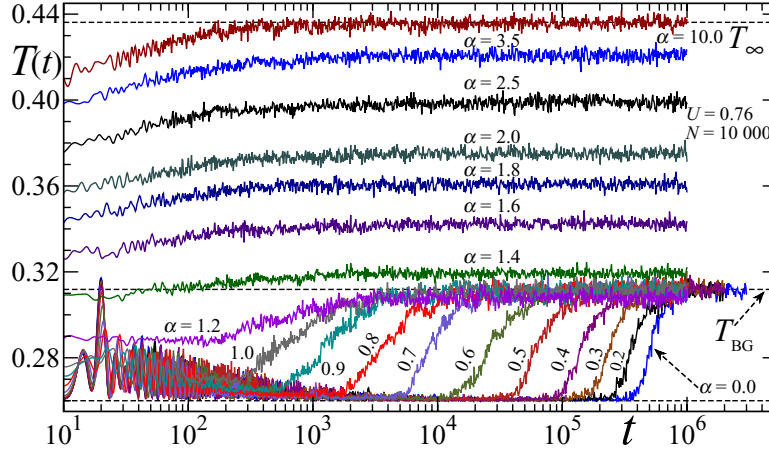
Figure 3. Time evolution of the kinetic temperature $T(t) = K(t)/N$ for a single realization of $N = 10\,000$ Heisenberg rotators defined by equation (1), with a total energy $U = 0.76$ and several values of the interaction-range parameter α. The upper horizontal dashed line, at $T_\infty \approx 0.4362$, represents the Boltzmann–Gibbs (BG) equilibrium temperature of the corresponding $\alpha \to \infty$ model (see equation (3)). The dashed horizontal line at $T_{\mathrm{BG}} \approx 0.3118$ indicates the BG equilibrium temperature for $0 \leqslant \alpha < 1$ (see equations (3) and (4)), whereas the lower horizontal line, at $T = U - 1/2 = 0.26$, corresponds to the QSS temperature characterized by zero magnetization. In the range $1 \leqslant \alpha < \infty$, no analytical solution is available, as far as we know. The time is dimensionless and each unit of (physical) time t corresponds to 50 iterations of the equations of motion.

At $\alpha \approx 1$ one notices a crossover from the existence of these metastable states to a smooth gradual increase in the kinetic temperature, such that for $\alpha > 1$ there is no clear evidence of QSSs. Finally, for a sufficiently high value of α (e.g. $\alpha = 10$), the long-time behaviour of the kinetic temperature $T(t)$ gradually approaches the BG equilibrium temperature of the corresponding $\alpha \to \infty$ model, i.e. the nearest-neighbour-interaction model ($T_\infty \approx 0.4362$). Our numerical results however do not exclude a possible finite-size dependence of these short-lived QSSs for $\alpha \gtrsim 1$, as already found in the α-XY case [40]. However, no dependence on N is expected for $\alpha \gg 1$, since the interaction potential becomes effectively short range in this limit.

An important question concerns the range of energies over which the above-mentioned QSSs exist. In figure 4 we present part of the caloric curve for $0 \leqslant \alpha < 1$, corresponding to energies $U \leqslant U_{\mathrm{c}}$ (full line). Numerical simulations for a single copy of $N = 10\,000$ rotators, in the cases $\alpha = 0.0, 0.4$ and 0.8, show that the QSSs characterized by $M = 0$ (symbols along the dashed line) exist within the range $0.70 \lesssim U < U_{\mathrm{c}}$, in agreement with the results of figure 2. However, as one goes further below the critical point, roughly for $0.50 < U < 0.70$, QSSs are still found numerically, although characterized by finite values of magnetization, in spite of the initial conditions of zero magnetization considered. Such states are understood due to the prevalence of the ferromagnetic couplings for sufficiently low values of U and they may be observed more clearly in the case $\alpha = 0.0$, being sometimes difficult to be identified for higher values of α (e.g. $\alpha = 0.80$). It should be
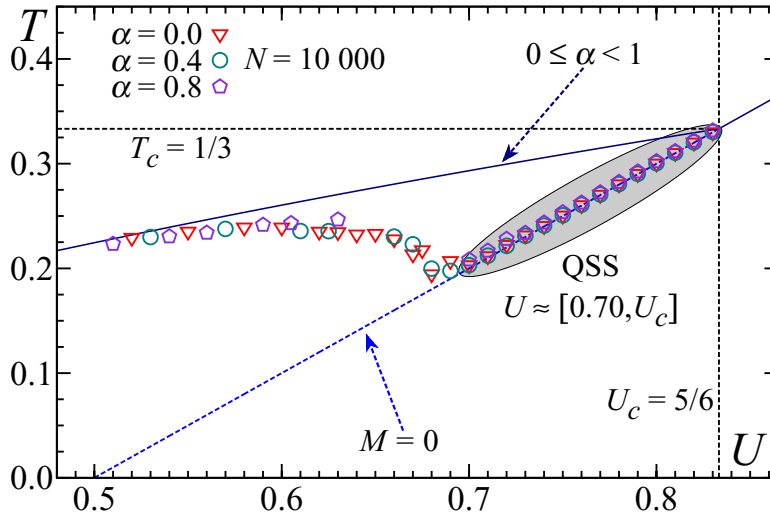
Figure 4. Part of the caloric curve for the cases $0 \leqslant \alpha < 1$ (see figure 1(a)) is exhibited for energies $U \leqslant U_c$ (full line). The range of energies over which QSSs were verified numerically is shown for both zero magnetization (dashed line), as well as for $M > 0$. The symbols correspond to data associated with the kinetic temperatures of the QSSs, obtained from numerical simulations for a single copy of a system composed by $N = 10\,000$ rotators, in the cases $\alpha = 0.0, 0.4$ and 0.8.

noticed that within a small energy range (typically $U \lesssim 0.70$), the QSSs yield a negative microcanonical specific heat. Although this represents a well-known feature for the HMF model (see discussion in [15]), it is the first time that such a result is verified for a system of Heisenberg rotators, to our knowledge. The numerical data of figure 4 suggests that a negative specific heat should occur for $0 \leqslant \alpha < 1$.

The most interesting feature of the QSSs presented in figures 2 and 3 concerns an increase in t_{QSS} for increasing N, as shown in figure 5, where we analyse the QSSs for an energy $U = 0.76$ in the cases $\alpha = 0.0, 0.4$ and 0.8, by varying the system sizes. It should be mentioned that, in order to identify QSSs clearly within the present approach, we had to simulate systems with sufficiently high values of N (essentially, $N = 2500$ or higher). Hence, in figure 5 such a behaviour is presented for typical values of N in the range from $N = 2500$ up to $N = 30000$, for the smaller values of α (i.e. $\alpha = 0.0$ and 0.4); however, in the case $\alpha = 0.8$ the observation of QSSs becomes more difficult, in such a way that one needs to simulate larger values of N (e.g. $N = 5000$ or higher) for this purpose. The growth of t_{QSS} for increasing N represents a well-known feature in models of rotators, like the HMF and α-XY (with $0 < \alpha < 1$) models [9–17, 24, 29, 30], as well as the inertial Heisenberg model [8, 26, 27], yielding significant physical consequences, some of them directly related to the applicability of BG statistical mechanics. More specifically, the order in which the thermodynamic limit ($N \to \infty$) and the infinite-time limit ($t \to \infty$) are considered becomes mostly relevant in the present case, in such a way that if the thermodynamic limit is carried first, one should remain in a QSS forever. This may be viewed as a breakdown of ergodicity, with the system being trapped in a QSS, never reaching the BG equilibrium state; consequently, time averages and ensemble averages do not coincide, violating a basic assumption of BG statistical mechanics. The QSS represents the final state in this case;
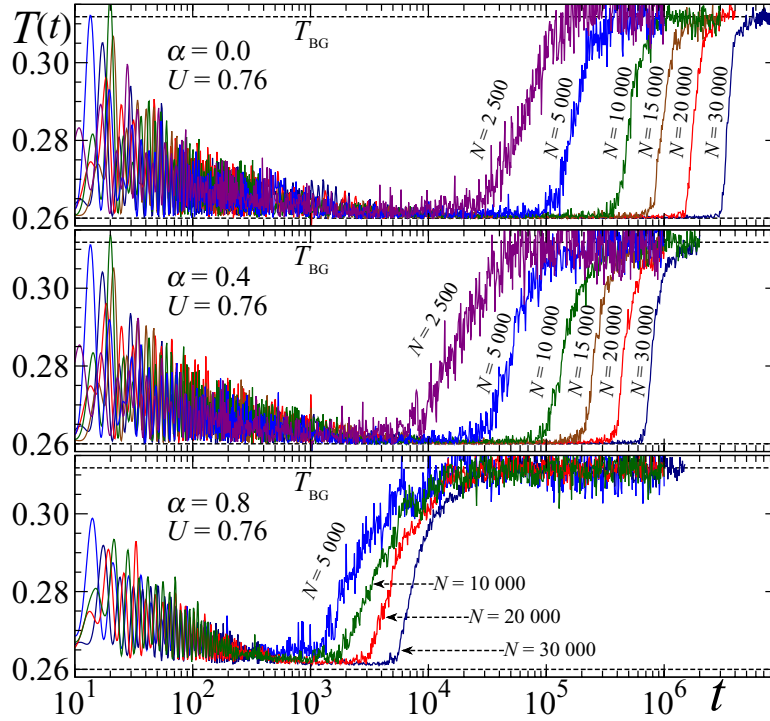
Figure 5. Typical QSSs presented in figures 2 and 3 are analysed for varying system sizes, showing an increase in their lifetime t_{QSS} as N increases.

whether it should be interpreted as a truly equilibrium thermodynamical one represents an important question beyond the scope of the present work.

Herein we have defined the duration t_{QSS} of a given QSS (e.g. those exhibited in figure 5), as the time at which $T(t)$ presents its halfway between the values at the QSS and its corresponding T_{BG}. The fact that we are computing this time interval starting from $t = 0$, including a short transient regime before reaching the QSS, does not affect our final results, since this small transient becomes negligible in the final computation of t_{QSS}, for sufficiently large values of N. According to this, the growth of t_{QSS} with the total number of rotators N, for a given energy ($U = 0.76$) and three typical values of α ($\alpha = 0.0, 0.4$ and 0.8), is exhibited in figure 6. In the three cases investigated, these behaviours are fitted by power laws, $t_{\mathrm{QSS}} \sim N^{\gamma}$ (as shown in the respective inset, where the same data is presented in a log–log representation), with the exponent γ decreasing as α increases, e.g. $\gamma \approx 1.69$ ($\alpha = 0.0$), $\gamma \approx 1.54$ ($\alpha = 0.4$) and $\gamma \approx 0.62$ ($\alpha = 0.8$). In the first case, our estimate agrees with the one of [27] (see also [41]), where $\gamma \approx 1.70$ was computed. Curiously, such an estimate has also been found numerically for QSSs of the HMF model, with similar initial conditions (zero magnetization) [10], being supported through analytical approaches in [16]. One should mention that in the case $\alpha = 0.8$ the QSSs are more difficult to be observed, appearing only for sufficiently high values of N, such that data points for smaller N are not exhibited. In spite of such difficulties, our simulations suggest that one should have $\gamma \to 0$ in the limit $\alpha \to 1$. Although relevant, it is not possible to propose a particular scaling behaviour describing the decrease of γ with respect to α, on the basis of the present numerical simulations. Such a scaling deserves
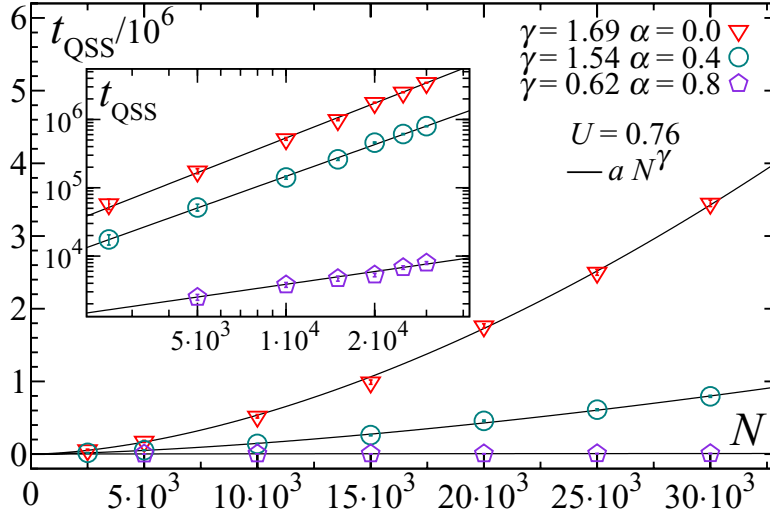
Figure 6. The growth of the lifetime of the QSSs (t_{QSS}) with respect to the size of the system is presented, for a fixed energy ($U = 0.76$) and three typical values of α ($\alpha = 0.0, 0.4$ and 0.8). Symbols correspond to data from numerical simulations, whereas full lines stand for the fits proposed. In the inset we exhibit the same data in a log–log representation.
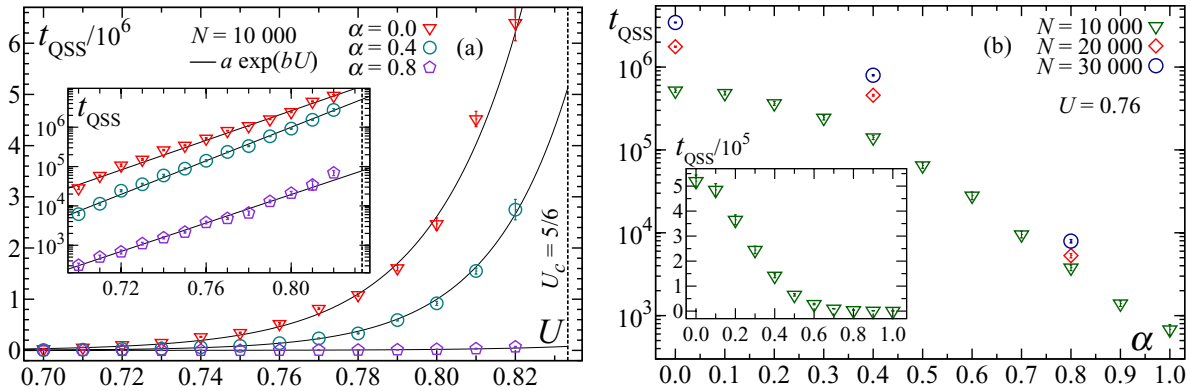

Figure 7. Behaviours of the lifetime of the QSSs (t_{QSS}), with respect to the energy U and to the interaction-range parameter α, are shown. (a) Fixed number of rotators ($N = 10\,000$), three typical values of α ($\alpha = 0.0, 0.4$ and 0.8), varying the energy in the range $0.70 \leqslant U < U_c$; the same data are exhibited in a log-linear representation in the inset. (b) Fixed energy ($U = 0.76$), three values for the total number of rotators ($N = 10\,000, 20\,000$ and $30\,000$), varying α in the range $0 \leqslant \alpha \leqslant 1$; the data for $N = 10\,000$ are exhibited in a linear–linear representation in the inset. Symbols correspond to data from numerical simulations of a single copy of the Hamiltonian in equation (1), whereas full lines stand for the fits proposed.

further computational efforts, from which one could obtain a larger number of data points for an appropriate plot of γ versus α (see, e.g. [42] for the XY case).

The behaviours of the duration t_{QSS} of the present QSSs with respect to the total energy U, as well as its decrease with the parameter α are presented in figure 7.

In figure 7(a) we exhibit data of simulations of $N = 10\,000$ rotators, for three values of α ($\alpha = 0.0, 0.4$ and 0.8), varying the energy in the range $0.70 \leqslant U < U_c$. These results show that t_{QSS} grows exponentially for increasing U in this range, as can be seen more clearly through the log-linear representation in the inset. Although t_{QSS} may become very large as $U \to U_c$, from the plots of figure 2 one sees that the gap between the kinetic temperature of each QSS and the equilibrium state, represented by T_{BG}, decreases as U approaches U_c. Hence, in this case, the QSSs disappear by means of the difference between these two quantities, which goes to zero as $U \to U_c$, so that for $U \gtrsim U_c$ one finds no QSSs. The dependence of t_{QSS} on the interaction-range parameter α ($0 \leqslant \alpha \leqslant 1$) is presented in figure 7(b), where we exhibit data of simulations for the energy $U = 0.76$ and three values for the total number of rotators ($N = 10\,000, 20\,000$ and $30\,000$). In the log-linear representation, one sees that these results do strongly depend on N, although they are all suggestive that $t_{QSS} \to 0$ as $\alpha \to 1$; more particularly, the linear–linear representation of the inset indicates this tendency more clearly in the case $N = 10\,000$.

4. Conclusions

We have carried molecular-dynamics simulations on a one-dimensional Hamiltonian system, composed by N classical localized Heisenberg rotators on a ring. We have considered the two-body interaction characterized by a distance r_{ij} between rotators at sites i and j, decaying with the distance r_{ij} as a power law, $1/r_{ij}^{\alpha}$ ($\alpha \geqslant 0$). In this way, one may control the range of the interactions by changing the parameter α and specially, two well-known cases may be recovered, namely, the fully-coupled (i.e. mean-field limit) and nearest-neighbour-interaction models, in the limits $\alpha = 0$ and $\alpha \to \infty$, respectively. For the first time in the literature, we have numerically established the validity of the correct scaling for spin dimensionality $n > 2$. Considering this scaling, one obtains the same thermodynamical behaviour for any α in the range $0 \leqslant \alpha < 1$, as analytically predicted in [28].

We have investigated the dynamics of the model by following the time evolution of a single copy of rotators, for energies U below its critical value ($U < U_c$), considering initial conditions corresponding to zero magnetization. Analogously to what happens for the similar model of XY rotators, we have verified the existence of quasi-stationary states (QSSs) for values of α in the range $0 \leqslant \alpha < 1$. But, in contrast to the XY rotators, the allowed number of initial conditions of the present model is substantially larger. The particular types of initial conditions that will lead the system to robust QSSs was discussed, representing a very relevant matter for further analytical investigations. For a given energy U, our numerical analysis indicated that the durations t_{QSS} grow by increasing N, following a power law, $t_{QSS} \sim N^{\gamma}$, where the exponent γ gets reduced for increasing values of α in the range $0 \leqslant \alpha < 1$; particularly, our results suggest that $\gamma \to 0$ as $\alpha \to 1$. The relevance of establishing the growth of t_{QSS} with N accurately, achieved herein by considering sufficiently large values of N, may be assessed if one takes into account the fact that in spite of the large amount of effort dedicated to the α-XY model, this matter is still controversial for this system (see, e.g. [16, 18]). The particular scaling behaviour, describing the decrease of γ with respect to α, requires further computational

efforts and is left for future investigations. Moreover, for the initial conditions and energy range considered, we have shown that the duration of the QSSs grows exponentially with the energy, $t_{\mathrm{QSS}} \sim \exp(bU)$, for N and α fixed. Our simulations have indicated that the gaps separating the kinetic temperature of these QSSs and their corresponding equilibrium temperatures T_{BG} become larger for smaller energies, dropping to zero as $U \to U_{\mathrm{c}}$. In this way, the QSSs disappear by means of the difference between these two quantities, which goes to zero as $U \to U_{\mathrm{c}}$, so that for $U \gtrsim U_{\mathrm{c}}$ one finds no QSSs.

We have found QSSs over a wide range of energies, typically for $0.50 < U < U_{\mathrm{c}}$ ($U_{\mathrm{c}} = 5/6$), although these states presented zero magnetization throughout a smaller interval, $0.70 \lesssim U < U_{\mathrm{c}}$. It should be mentioned that we have chosen to explore more deeply the QSSs associated with a given value of energy ($U = 0.76$), where such states could be observed easily through simulations of a single copy of rotators. However, the results presented herein for this particular energy should be valid for any similar QSS (characterized by zero magnetization) in the range $0.70 \lesssim U < U_{\mathrm{c}}$. By going further below the critical point, roughly for $0.50 < U < 0.70$, QSSs were still found numerically, but in contrast to the above-mentioned ones, they are characterized by finite values of magnetization, in spite of the initial conditions of zero magnetization considered. Within a small energy range (typically $U \lesssim 0.70$), the numerical data of the kinetic temperature of these QSSs versus U yielded a negative microcanonical specific heat. Although this represents a well-known feature for the HMF model, it is the first time that such a result has been verified for a system of Heisenberg rotators, to our knowledge.

The particular case $\alpha = 0.0$ of the present analysis (carried herein for the Cartesian components of angular momenta and spin variables), coincides precisely with the one of [27], which have considered angular variables and their corresponding canonically-conjugated angular momenta. Herein, we have extended these results for power-law decaying interactions among spin variables, by investigating situations characterized by $\alpha > 0$, showing that interesting QSSs appear for any α in the range $0 \leqslant \alpha < 1$. Due to the wide diversity of possibilities for initial conditions in both spins and angular momenta in the present model, investigations for QSSs under initial conditions different from the ones considered herein would be highly desirable.

Acknowledgments

References

[1] Nakamura T 1952 Statistical theory of hindered rotation in molecular crystals *J. Phys. Soc. Japan* **7** 264
Fisher M E 1964 Magnetism in one-dimensional systems–the Heisenberg model for infinite spin *Am. J. Phys.* **32** 343
[2] Joyce G S 1967 Classical Heisenberg model *Phys. Rev.* **155** 478
[3] Stanley H E 1969 Exact solution for a linear chain of isotropically interacting classical spins of arbitrary dimensionality *Phys. Rev.* **179** 570

[4] Stanley H E 1971 *Introduction to Phase Transitions and Critical Phenomena* (New York: Oxford University Press)

[5] Thompson C J 1988 *Classical Equilibrium Statistical Mechanics* (Oxford: Oxford University Press)

[6] Antoni M and Ruffo S 1995 Clustering and relaxation in Hamiltonian long-range dynamics *Phys. Rev.* E **52** 2361

[7] Anteneodo C and Tsallis C 1998 Breakdown of exponential sensitivity to initial conditions: role of the range of interactions *Phys. Rev. Lett.* **80** 5313

[8] Nobre F D and Tsallis C 2003 Classical infinite-range-interaction Heisenberg ferromagnetic model: metastability and sensitivity to initial conditions *Phys. Rev.* E **68** 036115

[9] Latora V, Rapisarda A and Tsallis C 2001 Non-Gaussian equilibrium in a long-range Hamiltonian system *Phys. Rev.* E **64** 056134

[10] Yamaguchi Y Y, Barré J, Bouchet F, Dauxois T and Ruffo S 2004 Stability criteria of the Vlasov equation and quasi-stationary states of the HMF model *Physica* A **337** 36

[11] Pluchino A, Latora V and Rapisarda A 2004 Glassy dynamics in the HMF model *Physica* A **340** 187

Pluchino A, Latora V and Rapisarda A 2006 Effective spin–glass Hamiltonian for the anomalous dynamics of the HMF model *Physica* A **370** 573

Pluchino A, Latora V and Rapisarda A 2004 Metastable states, anomalous distributions and correlations in the HMF model *Physica* D **193** 315

[12] Latora V, Rapisarda A and Ruffo S 1998 Lyapunov instability and finite size effects in a system with long-range forces *Phys. Rev. Lett.* **80** 692

Latora V, Rapisarda A and Ruffo S 1999 Chaos and statistical mechanics in the Hamiltonian mean field model, *Physica* D **131** 38

[13] Moyano L G and Anteneodo C 2006 Diffusive anomalies in a long-range Hamiltonian system *Phys. Rev.* E **74** 021118

[14] Pluchino A, Rapisarda A and Tsallis C 2007 Nonergodicity and central-limit behavior for long-range Hamiltonians *Europhys. Lett.* **80** 26002

Pluchino A, Rapisarda A and Tsallis C 2008 A closer look at the indications of q-generalized central limit theorem behavior in quasi-stationary states of the HMF model *Physica* A **387** 3121

[15] Chavanis P-H and Campa A 2010 Inhomogeneous Tsallis distributions in the HMF model *Eur. Phys. J.* B **76** 581

Campa A and Chavanis P-H 2013 Caloric curves fitted by polytropic distributions in the HMF model *Eur. Phys. J.* B **86** 1

[16] Ettoumi W and Firpo M-C 2013 Action diffusion and lifetimes of quasistationary states in the Hamiltonian mean-field model *Phys. Rev.* E **87** 030102

[17] Campa A, Dauxois T and Ruffo S 2009 Statistical mechanics and dynamics of solvable models with long-range interactions *Phys. Rep.* **480** 57

[18] Rocha Filho T M, Amato M A, Santana A E, Figueiredo A and Steiner J R 2014 Dynamics and physical interpretation of quasistationary states in systems with long-range interactions *Phys. Rev.* E **89** 032116

Rocha Filho T M, Santana A E, Amato M A and Figueiredo A 2014 Scaling of the dynamics of homogeneous states of one-dimensional long-range interacting systems *Phys. Rev.* E **90** 032133

[19] Jund P, Kim S G and Tsallis C 1995 Crossover from extensive to nonextensive behavior driven by long-range interactions *Phys. Rev.* B **52** 50

[20] Campa A, Giansanti A, Moroni D and Tsallis C 2001 Classical spin systems with long-range interactions: universal reduction of mixing *Phys. Lett.* A **286** 251

[21] Tamarit F and Anteneodo C 2000 Rotators with long-range interactions: connection with the mean-field approximation *Phys. Rev. Lett.* **84** 208

[22] Tsallis C 2009 *Introduction to Nonextensive Statistical Mechanics Approaching a Complex World* (New York: Springer)

[23] Campa A, Giansanti A and Moroni D 2000 Canonical solution of a system of long-range interacting rotators on a lattice *Phys. Rev.* E **62** 303

[24] Cirto L J L, Assis V R V and Tsallis C 2014 Influence of the interaction range on the thermostatistics of a classical many-body system *Physica* A **393** 286

[25] Firpo M-C and Ruffo S 2001 Chaos suppression in the large size limit for long-range systems *J. Phys. A: Math. Gen.* **34** L511

Anteneodo C and Vallejos R O 2001 Scaling laws for the largest Lyapunov exponent in long-range systems: a random matrix approach *Phys. Rev.* E **65** 016210

[26] Nobre F D and Tsallis C 2004 Metastable states of the classical inertial infinite-range-interaction Heisenberg ferromagnet: role of initial conditions *Physica* A **344** 587

[27] Gupta S and Mukamel D 2013 Quasistationarity in a model of long-range interacting particles moving on a sphere *Phys. Rev.* E **88** 052137

[28] Campa A, Giansanti A and Moroni D 2003 Canonical solution of classical magnetic models with long-range couplings *J. Phys. A: Math. Gen.* **36** 6897

[29] Campa A, Giansanti A and Moroni D 2002 Metastable states in a class of long-range Hamiltonian systems *Physica* A **305** 137

[30] Giansanti A, Moroni D and Campa A 2002 Universal behavior in the static and dynamic properties of the α-XY model *Chaos Solitons Fractals* **13** 407

[31] Tsallis C 1995 Nonextensive thermodynamics and fractals *Fractals* **03** 541

[32] Cannas S A and Tamarit F A 1996 Long-range interactions and nonextensivity in ferromagnetic spin models *Phys. Rev.* B **54** R12661
    Sampaio L C, de Albuquerque M P and de Menezes F S 1997 Nonextensivity and Tsallis statistics in magnetic systems *Phys. Rev.* B **55** 5611

[33] Grigera J R 1996 Extensive and non-extensive thermodynamics. A molecular dynamic test *Phys. Lett.* A **217** 47
    Curilef S and Tsallis C 1999 Critical temperature and nonextensivity in long-range interacting Lennard–Jones-like fluids *Phys. Lett.* A **264** 270

[34] Parsons J D 1977 Linear chain of classical spins with arbitrary isotropic nearest-neighbor interaction *Phys. Rev.* B **16** 2311

[35] Rapaport D C and Landau D P 1996 Critical dynamics of a dynamical version of the classical Heisenberg model *Phys. Rev.* E **53** 4696

[36] Robb D T, Reichl L E and Faraggi E 2003 Simulation of hysteresis in magnetic nanoparticles with Nosé thermostating *Phys. Rev.* E **67** 056130

[37] Barojas J, Levesque D and Quentrec B 1973 Simulation of diatomic homonuclear liquids *Phys. Rev.* A **7** 1092

[38] Evans D J 1977 On the representation of orientation space *Mol. Phys.* **34** 317
    Evans D J and Murad S 1977 Singularity free algorithm for molecular dynamics simulation of rigid polyato *Mol. Phys.* **34** 327

[39] Allen M P and Tildesley D J 1987 *Computer Simulation of Liquids* (Oxford: Oxford University Press)

[40] Turchi A, Fanelli D and Leoncini X 2011 Existence of quasi-stationary states at the long range threshold *Commun. Nonlinear Sci. Numer. Simul.* **16** 4718
    Ettoumi W and Firpo M-C 2011 Stochastic treatment of finite-N effects in mean-field systems and its application to the lifetimes of coherent structures *Phys. Rev.* E **84** 030103

[41] Gupta S and Mukamel D 2011 Quasistationarity in a model of classical spins with long-range interactions *J. Stat. Mech.* P03015

[42] Bachelard R and Kastner M 2013 Universal threshold for the dynamical behavior of lattice systems with long-range interactions *Phys. Rev. Lett.* **110** 170603